Magnitude Response Peak Detection and Control Using Balanced Model Reduction and Leakage to a Target

Kent D. Benson, *Student Member, IEEE*, and William A. Sethares

***Abstract*—Adaptive filters are often used in systems that need to adjust to unknown environments. Communication channels with frequency nulls, signals that lack energy in a frequency band, and transducers with a finite bandwidth present special problems since adaptive filters can develop a large gain at frequencies where excitation is lacking. Such magnitude response peaks can cause problems if unchecked. This paper suggests a procedure for detecting and controlling magnitude response peaks that uses a balanced model reduction technique to form a low-order IIR filter that approximates the performance of the filter. The poles are then studied to determine if magnitude response peaks are present. If a peak is detected, then "leakage to a target" is used to gradually reduce the peak with minimal effect on the equalizer's response at other frequencies. Several useful bounds on the equalizer frequency response magnitude are derived, and the frequency domain behavior of the leakage to a target algorithm is analyzed. A case study is provided.**

I. Introduction

MANY DEVICES incorporate adaptive stages to automatically adjust the operation of the system in unknown environments. By adapting to the specific operating environment, these systems tend to outperform systems with fixed parameters. Occasionally, however, the environment is so ill conditioned that the adaptive algorithm generates parameters that are in some way unacceptable. For instance, [1] demonstrates that FIR filter tap-weight magnitudes may drift to infinity when an underexcited signal is input into the LMS algorithm, and [2] demonstrates how quantization errors due to digital implementation of adaptive algorithms may accumulate and degrade performance. In certain communication and acoustic systems, situations may develop where the adaptive portion of a system tries to overcompensate for signals that lack energy at certain frequencies or in certain frequency bands. This overcompensation takes the form of a filter with large frequency response magnitudes at these frequencies or in these frequency bands. Thus, magnitude response peaks form in a filter's response at frequencies where the filter input signal has little or no power. These magnitude response peaks may cause severe problems if left uncorrected.

Manuscript received September 26, 1995; revised March 24, 1997. The associate editor coordinating the review of this paper and approving it for publication was Dr. Stephen M. McLaughlin.

K. D. Benson is with Tellabs Operations, Inc., Mishawaka, IN 46545 USA (e-mail: kbenson@trc.tellabs.com).

W. A. Sethares is with the Department of Electrical and Computer Engineering, University of Wisconsin, Madison, WI 53706 USA (e-mail: sethares@ece.wisc.edu).

Publisher Item Identifier S 1053-587X(97)07361-3.

Many communication systems use adaptive filters as equalizers to compensate for channel distortions. In some cases, the output of the channel may have little or no energy in certain frequency bands. This may occur either because the channel has nulls or because the channel input has no energy at these frequencies. In the first case, the equalizer attempts to compensate by forming a filter with large magnitude response peaks. A channel of this type is shown in Fig. 1 along with typical equalizer responses. Note that the peaks in the equalizer responses, which are created without poles, correspond to the channel nulls. In the second case, the desired output signal lacks energy at these frequencies; therefore, there is no impetus to form a peak. However, since there is no filter input at this frequency, there is no penalty if a peak forms. In cases such as this, quantization noise often causes peaks to form [2].

Fractionally spaced equalizers (FSE's) constitute another class of equalizers that experience a magnitude response peak problem, as shown in [3] and [4]. Since an FSE samples the input waveform at a rate higher than the symbol rate, there is no signal energy between $(1+\alpha)\pi/T$ and $2\pi/T'-(1+\alpha)\pi/T$, where

T symbol rate;
T' FSE sampling rate;
α rolloff factor.

Over time, magnitude response peaks may form.

Magnitude response peak problems also arise in systems incorporating acoustical components. Acoustic signals are bandlimited because human speech and hearing as well as the various transducers used in acoustical systems such as microphones and loudspeakers are bandlimited. In active noise cancellation systems, loudspeakers are used to generate acoustic waveforms to cancel out noise. The cost function being minimized and the fact that some of these generated sound waves propagate back to the input microphone creating a feedback loop causes instability [5], [6]. Some adaptive echo-cancellation systems suffer from low frequency growth. In these cases, tap-weight growth is driven by spurious noises. A voice-band echo canceller that develops magnitude response peaks in ranges where the input had little energy is discussed in [2]. Over time, the registers overflowed and the system had to be reset.

Magnitude response peaks can cause several problems. If the filter input statistics change so that the input contains energy at the magnitude response peak frequency, it will be

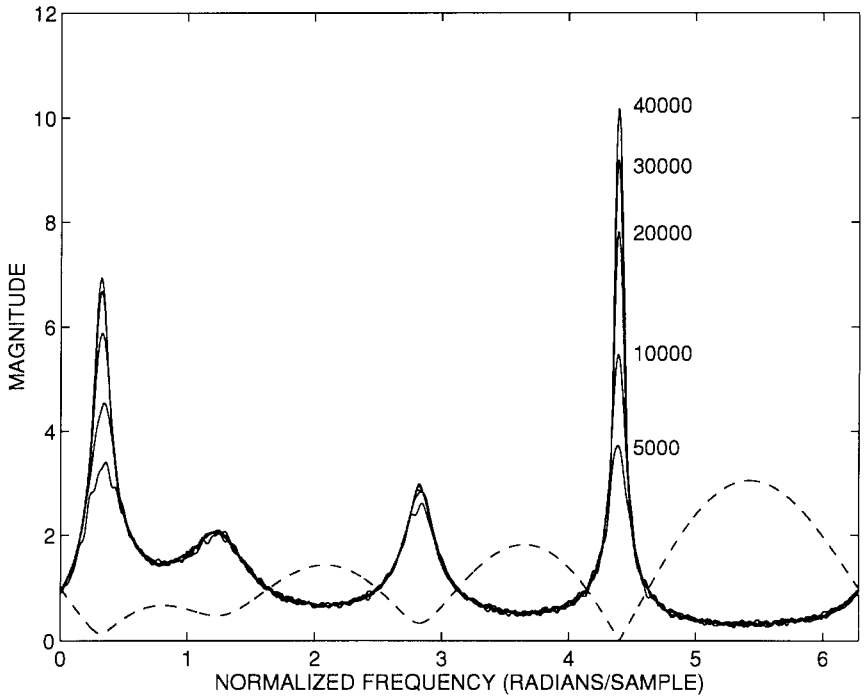

Fig. 1. Channel frequency response (dashed) and equalizer frequency responses (solid) at 5000, 10 000, 20 000, 30 000, and 40 000 iterations.

magnified to such a degree that the filter output becomes useless. Situations where the filter input can suddenly contain energy at the peak frequency include a time varying channel, where a channel null may move or disappear, and crosstalk, where an unwanted signal may suddenly appear at the filter input. Furthermore, for equalizers, a large filter response will amplify unwanted noise at the frequencies in question while failing to restore the lost frequency components. In addition, the registers storing the partial sums of the output or the filter weights may overflow. The filter may continue to operate with new, poorly set parameters or the overflow may cause an error that stops the operation of the equalizer. Finally, in the case of acoustic systems, a peak in the spectrum of the electrical signal controlling a loudspeaker can overdrive the loudspeaker, resulting in distortion and nonlinear effects.

In order to limit the effect of magnitude response peaks, a method is needed that will accomplish two tasks: It must detect when the response of the adaptive filter becomes too large, and it needs to counteract the rising response. This paper proposes a method that detects magnitude response peaks using a balanced model reduction technique to create a low-order IIR filter that approximates the behavior of the adaptive filter. By studying the poles of this IIR filter, the position of any magnitude response peaks can be determined. Magnitude response peaks are controlled using "leakage to a target." This variant of LMS biases the filter tap weights away from dangerous settings (that is, settings with a large magnitude response peak) and toward some more benign setting. This target weight vector can be formed by adding a strategically placed pole-zero pair to the steady-state filter.

The paper is organized as follows. Section II details the system setup and notational conventions. Section III describes the method of detecting magnitude response peaks using a balanced model reduction procedure. Section IV deals with and analyzes the control of the magnitude response peaks using leakage to a target. Section V discusses methods of reducing the computational cost of the detection process and derives bounds on the frequency response of the filter. Section VI illustrates the detection and control process and compares leakage to a target to several other methods of magnitude response peak control. Section VII concludes the paper.

II. System Setup

Consider the equalization formulation of an adaptive filter [7], [8] in which a complex valued signal $d(n)$ is distorted by an unknown, stable, minimum phase system to give $x(n)$. The quantity

$$y(n) = \sum_{i=1}^{M} a_i^*(n) d(n-i) + \sum_{i=0}^{N-1} b_i^*(n) x(n-i) \qquad (1)$$

is used to estimate $d(n)$ during the training phase, and the estimation error $e(n) = d(n) - y(n)$ is used to help identify the unknown parameters. During the decision directed phase, past filter outputs $y(n-i)$ are substituted for $d(n-i)$ in (1), forming an IIR filter. Observe that this formulation is equivalent to the equation error IIR system identification format [9] in which the identified system is inverted to form the equalizer. Defining the tap-weight and regressor vectors as

$$\mathbf{w}(n) = [a_1(n), a_2(n), \cdots, a_M(n), b_0(n) \; b_1(n), \cdots, b_{N-1}(n)]^T \qquad (2)$$

and

$$\mathbf{u}(n) = [d(n-1), d(n-2), \cdots, d(n-M) \; x(n), x(n-1), \cdots, x(n-N+1)]^T \qquad (3)$$

the filter output at time n can be written as $y(n) = \mathbf{w}^H(n)\mathbf{u}(n)$, where the superscript H is the complex transpose.

The statistical characteristics of these signals play an important role in the analysis of the filter. The autocorrelation of the regressor vector is given by $\mathbf{R} = E[\mathbf{u}(n)\mathbf{u}^H(n)]$, where $E[\cdot]$ is the expectation operator. $\mathbf{R}$ is assumed positive definite, which holds if the autocorrelation of the input vector $[x(n), \cdots, x(n-N+1)]^T$ is positive definite and if the numerator and denominator polynomials defined by the $a_i(n)$ and $b_i(n)$ coefficients are coprime and stable. See [10] for details. $\mathbf{R}$ can be written as $\mathbf{QDQ}^H$, where $\mathbf{Q}$ is a unitary matrix, and $\mathbf{D}$ is a diagonal matrix. Denoting the orthonormal eigenvectors of $\mathbf{R}$ as $\mathbf{v}_0, \mathbf{v}_1, \cdots, \mathbf{v}_{M+N-1}$, and the distinct real eigenvalues as $\lambda_0, \lambda_1, \cdots, \lambda_{M+N-1}$ (where λ_i is associated with the eigenvector v_i), then $\mathbf{Q} = [\mathbf{v}_0|\mathbf{v}_1|\cdots|\mathbf{v}_{M+N-1}]$, and $\mathbf{D} = \text{diag}\,(\lambda_0, \lambda_1, \cdots, \lambda_{M+N-1})$. The orthonormality of the eigenvectors implies $\mathbf{v}_i^H\mathbf{v}_j = \delta_{ij}$, which in turn implies that $\mathbf{Q}$ is unitary. The cross correlation between the received signal vector and the desired signal and variance of the desired signal are $\mathbf{p} = E[\mathbf{u}(n)d^*(n)]$ and $\sigma_d^2 = E[|d(n)|^2]$.

III. Detection of Magnitude Response Peaks via Balanced Model Reduction

Certain qualitative properties of the frequency response of a discrete-time filter can be determined by studying the locations of the filter's poles and zeros. For instance, if a pole lies very close to the unit circle, there may be a large peak in the magnitude of the filter's response. The effect of this pole may, however, be canceled by a nearby zero; therefore, the positions of the poles alone do not dictate the positions of magnitude response peaks. Furthermore, certain patterns involving a large number of zeros can also create large magnitude response peaks. For instance, the equalizer responses shown in Fig. 1 are not formed by poles (see Section VI for details). Such peaks are not easily identified from a pole-zero plot.

An alternative approach is to find a low-order IIR filter that closely approximates the frequency response of the equalizer. This new "filter" (which is never actually used to filter data but rather exists solely as mathematical model for the purposes of analysis) contains a small number of poles and zeros so that any poles or zeros that do not have a large effect on the filter response are eliminated. Thus, the poles of the low-order IIR filter will indicate the positions of the magnitude response peaks. The presence of a large magnitude response peak can be determined by checking if any of the poles of the IIR approximate filter lie near the unit circle, and the frequency of any magnitude response peaks can be determined from the locations of the poles.

A. Balanced Model Reduction—General Case

Balanced model reduction [11]–[13] provides a way to find a low-order approximation to a higher order system. Recall that any discrete-time, linear, time-invariant, lumped parameter, SISO system has a state space realization $[\mathbf{A}, \mathbf{B}, \mathbf{C}, \mathbf{D}]$ with a z-domain transfer function $F(z) = \mathbf{C}(z\mathbf{I}-\mathbf{A})^{-1}\mathbf{B}+\mathbf{D}$. The controllability grammian $\mathbf{P}$ and the observability grammian $\mathbf{Q}$ are defined as solutions to $\mathbf{APA}^H+\mathbf{BB}^H = \mathbf{P}$ and $\mathbf{A}^H\mathbf{QA}+\mathbf{C}^H\mathbf{C} = \mathbf{Q}$. For any nonsingular $\mathbf{T}$, a new state-space realization of the filter $[\overline{\mathbf{A}}, \overline{\mathbf{B}}, \overline{\mathbf{C}}, \overline{\mathbf{D}}] = [\mathbf{T}^{-1}\mathbf{AT}, \mathbf{T}^{-1}\mathbf{B}, \mathbf{CT}, \mathbf{D}]$ can be found with a transfer function

$$\overline{F}(z) = \overline{\mathbf{C}}(z\mathbf{I}-\overline{\mathbf{A}}^{-1})\overline{\mathbf{B}}+\overline{\mathbf{D}} = F(z). \tag{4}$$

It follows that $\overline{\mathbf{P}} = \mathbf{T}^{-1}\mathbf{P}(\mathbf{T}^H)^{-1}$ and $\overline{\mathbf{Q}} = \mathbf{T}^H\mathbf{QT}$. Observe that the eigenvalues of the product of $\mathbf{P}$ and $\mathbf{Q}$ $\lambda_i(\mathbf{PQ})$ are equal to the eigenvalues of the product of $\overline{\mathbf{P}}$ and $\overline{\mathbf{Q}}$, $\lambda_j(\overline{\mathbf{PQ}})$. The Hankel singular values of the transfer function $F(z)$ are defined as

$$\sigma_j[F(z)] = +\sqrt{\lambda_i(\mathbf{PQ})} \tag{5}$$

where the singular values are arranged in descending order (hence, the subscripts j and i may not match).

A system realization $(\overline{\mathbf{A}}, \overline{\mathbf{B}}, \overline{\mathbf{C}}, \overline{\mathbf{D}})$ is called a balanced if

$$\overline{\mathbf{P}} = \overline{\mathbf{Q}} = \mathbf{\Sigma} = \text{diag}\,(\sigma_1, \sigma_2, \cdots, \sigma_m). \tag{6}$$

A balanced realization is useful because reduced-order approximations can be found by merely selecting the leading states from $\overline{\mathbf{A}}$, $\overline{\mathbf{B}}$, $\overline{\mathbf{C}}$, and $\overline{\mathbf{D}}$ and discarding the remaining states. The Hankel singular values can be used as a valuable guide to how many states are necessary for a "good" approximation.

The main task involved in balanced model reduction consists of finding the transformation matrix $\mathbf{T}$ that transforms the original system realization $(\mathbf{A}, \mathbf{B}, \mathbf{C}, \mathbf{D})$ into the balanced realization $(\overline{\mathbf{A}}, \overline{\mathbf{B}}, \overline{\mathbf{C}}, \overline{\mathbf{D}})$. For systems that are stable, observable, and controllable, $\mathbf{P}$ and $\mathbf{Q}$ are positive definite, and $\mathbf{T}$ can be found in a fairly straightforward manner. $\mathbf{P}$ and $\mathbf{Q}$ can be factored as $\mathbf{P} = \mathbf{RR}^H$ and $\mathbf{Q} = \mathbf{S}^H\mathbf{S}$. The matrix $\mathbf{SPS}^H$ is symmetric and can be factored as $\mathbf{SPS}^H = \mathbf{SRR}^H\mathbf{S}^H = \mathbf{U\Sigma}^2\mathbf{U}^H$, where $\mathbf{UU}^H = \mathbf{I}$, which is the identity matrix. Finally, $\mathbf{T} = \mathbf{S}^{-1}\mathbf{U\Sigma}^{1/2}$. The number of operations required to perform a balanced realization depends greatly on the specific algorithm used [14], [15]. One popular procedure requires approximately $16(N-1)^3$ multiplications [14] (assuming $M \leq N-1$).

For the purposes of finding magnitude response peaks, the reduced-order approximation does not have to be particularly accurate at all frequencies. It only needs to closely approximate a filter at frequencies with large response magnitudes since these magnitude response peaks are the only phenomena of interest. A single-pole, single-zero IIR filter (found by keeping only a single state of the balanced realization) is preferable to an IIR filter with numerous poles and zeros since the single pole will coincide with the highest magnitude response peak. Thus, although a single pole filter may not model the entire frequency response of the original filter very well, it does contain the necessary information: the location of the largest magnitude response peak. One disadvantage of the single-pole, single-zero model is that it may not accurately represent the height of the magnitude response peak. [The error may be up to $2(\sigma_2+\sigma_3+\cdots+\sigma_{N-1})$, although it tends to be much smaller.] A solution to this problem is to use the current filter weights to find the true peak height at the known pole frequency. In this way, a single-pole, single-zero model can give accurate magnitude response peak information. In addition, the "danger

threshold" for large peaks can be specified directly in terms of the equalizer's response magnitude.

B. Balanced Model Reduction—FIR Case

For the special case of FIR filters, stability, controllability, and observability are assured as long as $b_{N-1} \neq 0$. Many of the matrices above can be calculated in advance since they are not functions of the tap weights and do not vary with time. In addition, the FIR structure causes many of these matrices to take on simple forms, many of which have been exploited in [16] for real-valued FIR filters. First, note that the state-space realization of an N-tap complex-valued FIR filter is

$$\mathbf{A} = \begin{bmatrix} 0 & 0 & 0 & \cdots & 0 & 0 \\ 1 & 0 & 0 & \cdots & 0 & 0 \\ 0 & 1 & 0 & \cdots & 0 & 0 \\ & & & \ddots & & \\ 0 & 0 & 0 & \cdots & 1 & 0 \end{bmatrix} \tag{7}$$

$$\mathbf{B} = [1, 0, 0, 0, \cdots, 0]^T, \tag{8}$$

$$\mathbf{C} = [b_1^*, b_2^*, b_3^*, \cdots, b_{N-2}^*, b_{N-1}^*] \text{ and } \mathbf{D} = b_0^*. \tag{9}$$

The Hankel matrix of the system is

$$\mathbf{H} = \begin{bmatrix} b_1^* & b_2^* & b_3^* & \cdots & b_{N-2}^* & b_{N-1}^* \\ b_2^* & b_3^* & b_4^* & \cdots & b_{N-1}^* & 0 \\ b_3^* & b_4^* & b_5^* & \cdots & 0 & 0 \\ \vdots & \vdots & \vdots & & \vdots & \vdots \\ b_{N-1}^* & 0 & 0 & \cdots & 0 & 0 \end{bmatrix} \tag{10}$$

where the tap weights' dependence on n has been suppressed for clarity. The controllability and observability grammians of the state-space filter realization in terms of the Hankel matrix are $\mathbf{P} = \mathbf{I}$ and $\mathbf{Q} = \mathbf{H}^H\mathbf{H}$.

The Hankel singular values of the system are $\sigma_i = +\sqrt{\lambda_i(\mathbf{H}^H\mathbf{H})}$. Notice that these are also the singular values of the Hankel matrix. Using the singular value decomposition (SVD) theorem, $\mathbf{H} = \mathbf{L}\mathbf{\Lambda}\mathbf{K}^H$, where $\mathbf{L}$ and $\mathbf{K}$ are unitary matrices, and $\mathbf{\Lambda} = \text{diag}\,(\sigma_1, \sigma_2, \cdots, \sigma_{N-1})$.

Now, let $\mathbf{R} = \mathbf{I}$ and $\mathbf{S} = \mathbf{\Lambda}\mathbf{K}^H$. To satisfy the theory developed for the general case, it is necessary that $\mathbf{P} = \mathbf{R}\mathbf{R}^H$ and $\mathbf{Q} = \mathbf{S}^H\mathbf{S}$. To see this, note that $\mathbf{R}\mathbf{R}^H = \mathbf{I}\mathbf{I}^H = \mathbf{I} = \mathbf{P}$, and

$$\begin{aligned} \mathbf{S}^H\mathbf{S} &= (\mathbf{\Lambda}\mathbf{K}^H)^H(\mathbf{\Lambda}\mathbf{K}^H) = (\mathbf{K}\mathbf{\Lambda}^H)(\mathbf{L}^H\mathbf{L})(\mathbf{\Lambda}\mathbf{K}^H) \\ &= (\mathbf{L}\mathbf{\Lambda}\mathbf{K}^H)^H(\mathbf{L}\mathbf{\Lambda}\mathbf{K}^H) = \mathbf{H}^H\mathbf{H} = \mathbf{Q}. \end{aligned} \tag{11}$$

The next task is to find $\mathbf{U}$ and $\mathbf{\Sigma}^2$ such that $\mathbf{S}\mathbf{P}\mathbf{S}^H = \mathbf{U}\mathbf{\Sigma}^2\mathbf{U}^H$. Observe that

$$\begin{aligned} \mathbf{U}\mathbf{\Sigma}^2\mathbf{U}^H &= \mathbf{S}\mathbf{P}\mathbf{S}^H = (\mathbf{\Lambda}\mathbf{K}^H)\mathbf{I}(\mathbf{\Lambda}\mathbf{K}^H)^H = \mathbf{\Lambda}\mathbf{K}^H\mathbf{K}\mathbf{\Lambda}^H \\ &= \mathbf{\Lambda}(\mathbf{K}^H\mathbf{K})\mathbf{\Lambda}^H = \mathbf{\Lambda}\mathbf{I}\mathbf{\Lambda} = \mathbf{\Lambda}^2. \end{aligned} \tag{12}$$

Therefore, taking $\mathbf{U} = \mathbf{I}$ and $\mathbf{\Sigma} = \mathbf{\Lambda}$ satisfies this requirement. Finally, these facts determine the transformation matrix

$$\begin{aligned} \mathbf{T} &= \mathbf{S}^{-1}\mathbf{U}\mathbf{\Sigma}^{1/2} = (\mathbf{\Lambda}\mathbf{K}^H)^{-1}(\mathbf{I})(\mathbf{\Lambda})^{1/2} \\ &= (\mathbf{K}^H)^{-1}(\mathbf{\Lambda}^{-1})(\mathbf{\Lambda}^{1/2}) = (\mathbf{K}\mathbf{\Lambda}^{-1})(\mathbf{\Lambda}^{1/2}) = \mathbf{K}\mathbf{\Lambda}^{-1/2}. \end{aligned} \tag{13}$$

For a general $(N-1) \times (N-1)$ matrix, finding $\mathbf{\Sigma}$ and $\mathbf{K}$ requires approximately $6(N-1)^3$ multiplications [17], [18]. For this specific application, the authors have found this estimate to be somewhat high, possibly due to the highly structured form of $\mathbf{H}$.

IV. Control of Magnitude Response Peaks via Leakage to a Target

Once a magnitude response peak has been detected, it is necessary to take steps to control it. The object is to reduce the magnitude of the system's frequency response at the frequency of the peak while leaving the rest of the frequency response unchanged. Standard leakage would reduce the magnitude response peak, but it would also reduce the response at nonpeak frequencies. One of the advantages of the system approximation method of peak detection discussed in the previous section is that the frequency of the magnitude response peak is known. Thus, a precise method of leaking away the magnitude response peak can be employed. This can be accomplished using "leakage to a target," where the target tap-weight vector has been chosen in such a way as to concentrate the effect of the leakage on the frequencies where the filter response is too large.

The strategy for the magnitude response peak reduction process is to find a target vector $\boldsymbol{\theta}$ that has a frequency response nearly identical to the frequency response of the current weight vector $\mathbf{w}(n)$, except in the critical region around the magnitude response peak. In this region, the target vector frequency response will have a magnitude lower than the magnitude of the frequency response of the current weight vector. This will cause the filter tap weights to have a response close to ideal over the range of frequencies where there is no trouble. The magnitude response of the filter tap weights will slowly leak toward the target vector over the frequency range where the response is dangerously large.

A. Leakage to a Target

One of the most common adaptive algorithms is the least mean squares (LMS) algorithm [19], which minimizes the squared error cost

$$J_{\text{LMS}}(n) = |e(n)|^2 = |d(n) - \mathbf{w}^H(n)\mathbf{u}(n)|^2. \tag{14}$$

This leads to the algorithm

$$\mathbf{w}(n+1) = \mathbf{w}(n) + \mu\mathbf{u}(n)e^*(n). \tag{15}$$

The tap-weight vector that minimizes this cost and is the steady-state solution to this algorithm is the minimum mean-squared error (MMSE) tap-weight vector $\mathbf{w}_o = \mathbf{R}^{-1}\mathbf{p}$.

Leakage to a target (LTAT) [20] is a generalization of LMS that augments the LMS cost function with a term that penalizes tap weights that differ from some fixed target tap weight $\boldsymbol{\theta}$.

$$J_{\text{LTAT}}(n) = |e(n)|^2 + [\mathbf{w}(n) - \boldsymbol{\theta}]^H\mathbf{\Gamma}[\mathbf{w}(n) - \boldsymbol{\theta}] \tag{16}$$

where $\mathbf{\Gamma} = \text{diag}\,(\gamma_0, \cdots, \gamma_{M+N-1})$, and γ_i are all real and nonnegative. Note that the target must have the same number

of tap weights as the filter. The leakage to a target tap-weight adaptation is

$$\mathbf{w}(n+1) = (\mathbf{I} - \mu\mathbf{\Gamma})\mathbf{w}(n) + \mu\mathbf{\Gamma}\boldsymbol{\theta} + \mu\mathbf{u}(n)e^*(n) \quad (17)$$

which biases the tap weights toward the target vector $\boldsymbol{\theta}$. The standard leakage algorithm [3], [4], [21] can be thought of as LTAT where the target vector is $\boldsymbol{\theta} = \mathbf{0}$ (the null vector) and $\gamma_i = \gamma \forall i$. That is, the leakage algorithm biases each of the tap weights toward zero. Setting $\mathbf{\Gamma} = \mathbf{0}$ reduces the LTAT algorithm to the standard LMS algorithm. Finally, note that the term $\mu\mathbf{\Gamma}\boldsymbol{\theta}$ does not vary with time. Once it has been calculated, the LTAT algorithm requires the some number of multiplications as standard leakage.

B. Optimal Tap-Weight Vector Under LTAT

With LTAT, the steady-state tap-weight vector for the filter will no longer be the MMSE tap-weight setting. Rather, the tap weights will now move toward $\mathbf{w}_T$, which is the set of steady-state tap weights that minimize the new average cost

$$\begin{aligned} J_{\mathrm{LTAT}}(\mathbf{w}) &= E[|e(n)|^2 + (\mathbf{w}-\boldsymbol{\theta})^H\mathbf{\Gamma}(\mathbf{w}-\boldsymbol{\theta})] \\ &= E[|d(n)|^2] - E[\mathbf{w}^H\mathbf{u}(n)d^*(n)] \\ &\quad - E[d(n)\mathbf{u}^H(n)\mathbf{w}] + E[\mathbf{w}^H\mathbf{u}(n)\mathbf{u}^H(n)\mathbf{w}] \\ &\quad + \mathbf{w}^H\mathbf{\Gamma}\mathbf{w} - \mathbf{w}^H\mathbf{\Gamma}\boldsymbol{\theta} - \boldsymbol{\theta}^H\mathbf{\Gamma}\mathbf{w} + \boldsymbol{\theta}^H\mathbf{\Gamma}\boldsymbol{\theta} \\ &= [\mathbf{w} - (\mathbf{R}+\mathbf{\Gamma})^{-1}(\mathbf{p}+\mathbf{\Gamma}\boldsymbol{\theta})]^H[\mathbf{R}+\mathbf{\Gamma}] \\ &\quad \cdot [\mathbf{w} - (\mathbf{R}+\mathbf{\Gamma})^{-1}(\mathbf{p}+\mathbf{\Gamma}\boldsymbol{\theta})] + [\sigma_d^2 + \boldsymbol{\theta}^H\mathbf{\Gamma}\boldsymbol{\theta}] \\ &\quad - (\mathbf{p}+\mathbf{\Gamma}\boldsymbol{\theta})^H(\mathbf{R}+\mathbf{\Gamma})^{-1}(\mathbf{p}+\mathbf{\Gamma}\boldsymbol{\theta}). \end{aligned} \quad (18)$$

The quantity $\mathbf{R}+\mathbf{\Gamma}$ is positive definite, and the last two terms on the right-hand side of (18) do not depend on the tap-weight vector. Thus, the tap-weight vector that causes the first term to be zero minimizes the cost. Therefore, (18) is minimized when

$$\mathbf{w} = \mathbf{w}_T = (\mathbf{R}+\mathbf{\Gamma})^{-1}(\mathbf{p}+\mathbf{\Gamma}\boldsymbol{\theta}). \quad (19)$$

This tap-weight vector can be expressed in terms of the MMSE tap-weight vector and a bias term. Using the matrix inversion lemma, $(\mathbf{R}+\mathbf{\Gamma})^{-1} = \mathbf{R}^{-1} - \mathbf{R}^{-1}(\mathbf{R}^{-1}+\mathbf{\Gamma}^{-1})^{-1}\mathbf{R}^{-1}$. Multiplying this expression by $(\mathbf{p}+\mathbf{\Gamma}\boldsymbol{\theta})$ and recalling that $\mathbf{R}^{-1}\mathbf{p} = \mathbf{w}_o$ is the MMSE tap-weight vector gives

$$\mathbf{w}_T = \mathbf{w}_o + \mathbf{R}^{-1}\mathbf{\Gamma}\boldsymbol{\theta} - \mathbf{R}^{-1}(\mathbf{R}^{-1}+\mathbf{\Gamma}^{-1})^{-1}\mathbf{R}^{-1}(\mathbf{p}+\mathbf{\Gamma}\boldsymbol{\theta}). \quad (20)$$

C. LTAT in the Frequency Domain—FIR Case

Frequency domain interpretations of signals and systems provide valuable insight into signal processing phenomena. This is especially true for the magnitude response peak problem since the existence of a potentially dangerous tap-weight setting can easily be observed as a large peak in the magnitude response of the equalizer. Adaptive filters, however, do not have a traditional frequency response because they are time varying. At any time, however, a "snapshot" of an adaptive filter's frequency response can be found by assuming that the current tap-weight vector is the tap-weight vector of a fixed filter. A series of such snapshots $F(\omega, n)$ can be used to study the evolution of an adaptive filter in the "frequency domain."

In the FIR filter case ($M = 0$), it is instructive to compare the frequency responses of the steady-state tap-weight vector of the standard LMS algorithm [which minimizes the mean-square error (MSE)] with the steady-state tap-weight vector of LTAT (which minimizes a trade-off between the MSE and the difference from a target tap-weight vector). This comparison can be made by using techniques presented in [22] and [23]. These papers show how a filter's frequency response can be studied in terms of the filter input autocorrelation eigenvectors. An FIR filter that uses one of the input's autocorrelation eigenvectors as a tap-weight vector is known as an eigenfilter.

Any FIR filter tap-weight vector can be written as a weighted sum of eigenvectors. This is possible because the set of N eigenvectors forms a basis for the N-dimensional complex vector space. Thus, any tap-weight vector $\mathbf{f}$ of length N can be written in this basis as

$$\mathbf{f} = \sum_{i=0}^{N-1} F_i^*\mathbf{v}_i \quad (21)$$

where

$$F_i = (\mathbf{v}_i^H\mathbf{f})^* = \mathbf{f}^H\mathbf{v}_i. \quad (22)$$

The frequency response of any set of N tap weights can be found by letting the tap weights act on the frequency vector $\mathbf{s}(\omega) = [1, \exp(-j\omega), \exp(-j2\omega), \cdots, \exp(-j(N-1)\omega)]^T$. For instance, the frequency response of the ith eigenfilter is $V_i(\omega) = \mathbf{v}_i^H\mathbf{s}(\omega)$. The frequency response of a filter with a tap-weight vector $\mathbf{f}$ is

$$\begin{aligned} F(\omega) &= \mathbf{f}^H\mathbf{s}(\omega) = \left[\sum_{i=0}^{N-1} F_i^*\mathbf{v}_i\right]^H \mathbf{s}(\omega) \\ &= \left[\sum_{i=0}^{N-1} F_i\mathbf{v}_i^H\right]^H \mathbf{s}(\omega) = \sum_{i=0}^{N-1} F_i\mathbf{v}_i^H\mathbf{s}(\omega) \\ &= \sum_{i=0}^{N-1} F_iV_i(\omega). \end{aligned} \quad (23)$$

Thus, the frequency response of any FIR filter with N weights can be decomposed into a weighted sum of eigenfilter frequency responses.

Frequency domain techniques can also be used to study an adaptive FIR filter as it converges to its steady-state configuration. Let the error-weight vector be

$$\boldsymbol{\epsilon}(n) = \mathbf{w}(n) - \mathbf{w}_o. \quad (24)$$

The average behavior of this error can be studied in the frequency domain (after making an appropriate assumption such as μ being small) by examining the frequency response of the error-weight vector $E(\omega, n) = \boldsymbol{\epsilon}^H(n)\mathbf{s}(\omega)$ (do not confuse this capital ϵ with the expectation operator), which is merely the difference between the filter frequency response at time n and the MMSE response. As shown in [22], this frequency domain representation of the error at time n can be written as

$$E(\omega, n) = \sum_{i=0}^{N-1} (1-\mu\lambda_i)^n\boldsymbol{\epsilon}^H(0)\mathbf{v}_iV_i(\omega). \quad (25)$$

The value $(1-\mu\lambda_i)$ determines how fast the error associated with each eigenfilter is reduced. That is, it determines how fast the weight coefficient of each eigenfilter converges to its steady-state weight value. Note that eigenfilter weights associated with large eigenvalues converge toward their steady-state values at a faster rate than the eigenfilter weights associated with small eigenvectors. Furthermore, eigenfilters tend to have a bandpass shape in the frequency domain, and the size of an eigenfilter's eigenvalue is related to the amount of input power in the frequency of the eigenfilter's "passband" [22]. Thus, the frequency response of an adaptive filter tends to converge to the optimal frequency response quickly in frequency bands with a large amount of input power. In contrast, a filter's frequency response tends to converge slowly in frequency bands with small amounts of input power. Thus, magnitude response peaks in the equalizer response, which correspond to frequencies with small amounts of input power, tend to form slowly, well after the rest of the frequency response has reached steady-state values.

These ideas are now applied to find the frequency response of various FIR tap-weight vectors.

Theorem 1: Let the regressor autocorrelation be $\mathbf{R} = \mathbf{Q}\mathbf{D}\mathbf{Q}^H$. If the filter's tap-weight vector can be defined as

$$\mathbf{f} = (\mathbf{Q}\mathbf{E}\mathbf{Q}^H)^{-1}\mathbf{r} \tag{26}$$

where $\mathbf{E} = \text{diag}\,(\rho_0, \rho_1, \cdots, \rho_{N-1})$ and $\mathbf{r}$ is a length-N column vector, then $F_i = \mathbf{r}^H\mathbf{v}_i/\rho_i^*$.

Proof: The complex conjugate of F_i can be written as

$$\begin{aligned} F_i^* &= \mathbf{v}_i^H\mathbf{f} = \mathbf{v}_i^H(\mathbf{Q}\mathbf{E}\mathbf{Q}^H)^{-1}\mathbf{r} = \mathbf{v}_i^H\mathbf{Q}\mathbf{E}^{-1}\mathbf{Q}^H\mathbf{r} \\ &= \mathbf{v}_i^H[\mathbf{v}_0|\cdots|\mathbf{v}_i|\cdots|\mathbf{v}_{N-1}]\mathbf{E}^{-1}\mathbf{Q}^H\mathbf{r} \\ &= [\mathbf{v}_i^H\mathbf{v}_0, \cdots, \mathbf{v}_i^H\mathbf{v}_i, \cdots, \mathbf{v}_i^H\mathbf{v}_{N-1}]\mathbf{E}^{-1}\mathbf{Q}^H\mathbf{r} \\ &= \left[0, \cdots, \frac{1}{\rho_i}, \cdots, 0\right]\mathbf{Q}^H\mathbf{r} \\ &\qquad \text{by the definition of } \mathbf{E} \text{ and } \mathbf{v}_i \\ &= \left(\frac{\mathbf{v}_i^H}{\rho_i}\right)\mathbf{r} = \frac{\mathbf{v}_i^H\mathbf{r}}{\rho_i}. \end{aligned} \tag{27}$$

□

The first weight vector to be analyzed is MMSE weight vector $\mathbf{w}_o = \mathbf{R}^{-1}\mathbf{p} = (\mathbf{Q}\mathbf{D}\mathbf{Q}^H)^{-1}\mathbf{p}$. In this case, Theorem 1 can be applied with $\mathbf{E} = \mathbf{D} = \text{diag}\,(\lambda_0, \lambda_1, \cdots, \lambda_{N-1})$, and $\mathbf{r} = \mathbf{p}$ giving $F_i^o = \mathbf{p}^H\mathbf{v}_i/\lambda_i$. Thus, each eigenfilter weight is inversely proportional to its corresponding eigenvalue. As mentioned before, each eigenvalue is related to the amount of power in the equalizer input in the passband of the corresponding eigenvector. These observations give rise to an excellent eigenfilter interpretation of how and why magnitude response peaks form. Assume that a channel null (or some other factor) results in there being very little power in the equalizer input signal at some frequency. The lack of input power at this frequency causes the eigenvalue corresponding to the eigenfilter with a passband at this frequency to be very small. This in turn leads to a large eigenfilter weight. This large weight causes the corresponding eigenfilter to dominate the frequency response of the equalizer [given by (23)]. Thus, the eigenfilter corresponding to the frequency of the channel null forms the resulting magnitude response peak. [The Appendix contains several derivations of an expression for the MMSE eigenfilter weights in terms of the unrestrained (any order) optimal tap-weight vector.]

For LTAT, the steady-state tap-weight vector is $\mathbf{w}_T = (\mathbf{R}+\mathbf{\Gamma})^{-1}(\mathbf{p}+\mathbf{\Gamma}\boldsymbol{\theta})$. In order to apply Theorem 1, the quantity $\mathbf{R}+\mathbf{\Gamma}$ can be written $\mathbf{R}+\mathbf{\Gamma} = \mathbf{Q}\mathbf{D}\mathbf{Q}^H + \mathbf{Q}\mathbf{\Gamma}\mathbf{Q}^H = \mathbf{Q}[\mathbf{D}+\mathbf{\Gamma}]\mathbf{Q}^H$. Thus, letting $\mathbf{E} = \mathbf{D}+\mathbf{\Gamma} = \text{diag}\,(\lambda_0+\gamma_0, \lambda_1+\gamma_1, \cdots, \lambda_{N-1}+\gamma_{N-1})$ and $\mathbf{r} = \mathbf{p}+\mathbf{\Gamma}\boldsymbol{\theta}$, Theorem 1 can be invoked to yield

$$\begin{aligned} F_i^T &= \frac{(\mathbf{p}+\mathbf{\Gamma}\boldsymbol{\theta})^H\mathbf{v}_i}{(\lambda_i+\gamma_i)^*} = \frac{\mathbf{p}^H\mathbf{v}_i}{\lambda_i+\gamma_i} + \frac{\boldsymbol{\theta}^H\mathbf{\Gamma}\mathbf{v}_i}{\lambda_i+\gamma_i} \\ &= \frac{\lambda_i}{\lambda_i+\gamma_i}F_i^o + \frac{\boldsymbol{\theta}^H\mathbf{\Gamma}\mathbf{v}_i}{\lambda_i+\gamma_i}. \end{aligned} \tag{28}$$

For the common special case of $\mathbf{\Gamma} = \text{diag}\,(\gamma, \cdots, \gamma)$

$$\begin{aligned} F_i^T &= \frac{(\mathbf{p}+\gamma\boldsymbol{\theta})^H\mathbf{v}_i}{(\lambda_i+\gamma)^*} = \frac{\mathbf{p}^H\mathbf{v}_i}{\lambda_i+\gamma} + \frac{\gamma\boldsymbol{\theta}^H\mathbf{v}_i}{\lambda_i+\gamma} \\ &= \frac{\lambda_i}{\lambda_i+\gamma}F_i^o + \frac{\gamma}{\lambda_i+\gamma}F_i^\theta \end{aligned} \tag{29}$$

where the target eigenfilter weights can be written as $F_i^\theta = \boldsymbol{\theta}^H\mathbf{v}_i$. Using this decomposition the effect of the well-known observation [4] that leakage in essence increase the eigenvalues of the input autocorrelation matrix can be observed directly. For a small λ_i, the addition of γ_i to the denominators in (28) will greatly reduce the eigenfilter weight. This will cause the corresponding eigenfilter to be less of a dominating factor in the equalizer frequency response, thereby reducing the magnitude response peak. Defining $\alpha_i = \lambda_i/(\lambda_i+\gamma)$, the steady-state frequency response of the filter under LTAT (for $\gamma_i = \gamma$) can be expressed in terms of the eigenfilters, the MMSE eigenfilter weights, the target eigenfilter weights, and the leakage factor. More explicitly

$$F^T(\omega) = \sum_{i=0}^{N-1}[\alpha_i F_i^o + (1-\alpha_i)F_i^\theta]V_i(\omega). \tag{30}$$

In particular, this demonstrates that LTAT has almost no effect on the frequency response in the region where the target and MMSE responses agree. Alternatively, in the region where they disagree, the effect is to slide the frequency response away from the MMSE response toward the target response in direct proportion to the size of α_i, which should be chosen large enough to reduce the magnitude response peak but not so large as to prevent the system from adapting to a time-varying channel.

LTAT is preferable to simply replacing the filter with the target tap-weight vector since the abruptness of completely changing tap weights will cause transients to develop. Furthermore, the use of target tap weights that add energy only in the amounts needed at each frequency ensures that the system can still respond to a change in the channel by changing the frequency response of the filter. The added term is weak enough to allow the system to adapt to most channel variations.

D. Finding Target Tap Weights

The problem has now been reduced to finding a set of target tap weights that have a frequency response close to the current

response at most frequencies but less than the current response magnitude at the frequency of a magnitude response peak. This can be accomplished using a notch filter, which is a pole-zero pair placed such that the pole and zero cancel each other out at frequencies where there is not a problem, yet reduces the magnitude of the peak. Such a pole-zero pair will change the frequency response at a given frequency by a factor equal to the distance from the unit circle (at an angle corresponding to the given frequency) to the new zero divided by the distance from the unit circle to the new pole.

To quantify this effect, assume that the pole lies a distance d_p from the origin, and the zero lies a distance d_z from the origin, both at an angle corresponding to the frequency of the peak. Let ϕ equal the distance, measured along the unit circle in normalized frequency, that a given normalized frequency ω is from the frequency of the magnitude response peak. For a point on the unit circle at an angle corresponding to the frequency ω, the distances from the point to the pole and zero are

$$\begin{aligned}&\text{distance (point to pole)}\\&\quad=\{[\cos(\phi)-d_p]^2+\sin^2(\phi)\}^{1/2}\\&\quad=[1-2d_p\cos(\phi)+d_p^2]^{1/2}\end{aligned}\tag{31}$$

and

$$\begin{aligned}&\text{distance (point to zero)}\\&\quad=\{[\cos(\phi)-d_z]^2+\sin^2(\phi)\}^{1/2}\\&\quad=[1-2d_z\cos(\phi)+d_z^2]^{1/2}.\end{aligned}\tag{32}$$

Defining the error ratio at any angle ϕ as the relationship between the old and new frequency response magnitudes $|H_{new}(\omega)|=\text{er}(\phi)|H_{old}(\omega)|$, this relationship can be written as

$$\begin{aligned}\text{er}(\phi)&=\frac{\text{distance (point to zero)}}{\text{distance (point to pole)}}\\&=\left[\frac{1-2d_z\cos(\phi)+d_z^2}{1-2d_p\cos(\phi)+d_p^2}\right]^{1/2}.\end{aligned}\tag{33}$$

For example, consider $d_z=0.9612$ and $d_p=0.9417$. Since $\text{er}(0)=2/3$, the peak is reduced by a factor of 1/3. The maximum error ratio (which always occurs at π rad/sample) is 1.01; therefore, the new response is at most only 1% larger than the original. Closer to the peak frequency, the new response is 99% of the original response at frequencies corresponding to angles only 0.1566 rad/sample from the peak frequency angle.

A pole-zero pair can be added to an IIR filter easily, but the process increases the number of coefficients by two. Discarding two coefficients creates a target tap-weight vector of the correct dimension. Adding a pole-zero pair to an FIR filter can be accomplished by using a pair of simple recursions, although the new tap-weight vector will have to be truncated to the correct length. Let the current filter have a magnitude response peak at the normalized frequency ω_p and a z transform

$$F(z)=b_0^*+b_1^*z^{-1}+b_2^*z^{-2}+\cdots+b_{N-1}^*z^{-(N-1)}.\tag{34}$$

If the z-domain location of the zero is α and the z-domain location of the pole is β, the zero has a z transform $Z(z)=1-\alpha z^{-1}$, and the pole has a z transform of $P(z)=1/(1-\beta z^{-1})$. For the situations described earlier, $\alpha=d_z\exp(j\omega_p)$, and $\beta=d_p\exp(j\omega_p)$. The new filter has a z transform $F'(z)=F(z)Z(z)P(z)$. Let c_i, $i=0,\cdots,N$ be the tap weights of $F(z)P(z)$. First, $c_0=b_0^*$. For $i=1,\cdots,N$, $c_i=b_i^*-\alpha b_{i-1}^*$ (where $b_N=0$). Now

$$\begin{aligned}F'(z)&=c_0+(c_1+\beta c_0)z^{-1}+[c_2+\beta(c_1+\beta c_0)]z^{-2}\\&\quad+\{c_3+\beta[c_2+\beta(c_1+\beta c_0)]\}z^{-3}+\cdots\\&=d_0+d_1z^{-1}+d_2z^{-2}+\cdots+d_{N-1}z^{-(N-1)}\\&\quad+d_Nz^{-N}+\cdots.\end{aligned}\tag{35}$$

These coefficients can be calculated via a simple recursion and then truncated to the desired order N. The coefficients are given by

1) $d_0=c_0$;
2) $i=1$;
3) $d_i=c_i+\beta d_{i-1}$;
4) $i=i+1$, go to 3.

This algorithm takes $c_i=0$ for $i>N$. The target tap-weight vector is $\boldsymbol{\theta}=[d_0^*,d_1^*,\cdots,d_{N-1}^*]^T=[d_0,d_1,\cdots,d_{N-1}]^H$, which gives an N-term FIR filter that closely approximates the original filter at all frequencies except those near the magnitude response peak where it has a lower response.

V. Reducing the Computational Load

One way to reduce the computational load of the detection procedure is to find the reduced order model only occasionally and to perform the model reduction calculations parallel to the normal tap-weight update calculations. This is possible because the frequency response of the filter changes slowly in the region of the peak. To see this, recall the frequency domain convergence results, and consider the peak and nonpeak frequencies separately. Frequencies with a small amount of input power are associated with slow convergence. Since a magnitude response peak forms at a frequency with little input power, the peak forms slowly. Thus, even if the model reduction calculations take place over multiple iterations of the adaptive algorithm, the magnitude of the peak response will not have changed significantly. Nonpeak frequencies have larger input power so that the response at these frequencies converges quickly and will be near the steady-state values by the time a peak has formed. Even if it takes several iterations to calculate the reduced order model of the system, the nonpeak frequencies will not have changed significantly. Thus, if the model reduction calculations are done parallel to the normal tap-weight update calculations, the model will be reasonably accurate, even though it is based on tap weights that are several iterations old. For example, by finding the balanced model once every N iterations and spreading the calculations evenly over this period, this procedure can be accomplished at a computational cost on the order of N^2 operations per iteration.

Another way to reduce the computational load of balanced model reduction is to avoid calculating it. This section gives three bounds on the peak frequency response magnitude. If any

TABLE I
PEAK MAGNITUDE RESPONSE AND MAGNITUDE RESPONSE BOUNDS

Iterations	Peak Magnitude	$\sum \lvert b_k(n) \rvert$	$2\sigma_1 + \lvert b_0 \rvert$	$2(\sigma_1 + \cdots + \sigma_{N-1})$
5000	3.7238	5.6935	4.3908	15.1448
10000	5.4634	7.5673	6.2757	17.2384
20000	7.8033	10.1115	8.8529	21.4282
30000	9.1515	11.6372	10.5389	24.8219
40000	10.1546	12.6073	11.7609	26.7663

of these bounds lie below the cut-off threshold for a dangerous magnitude response peak, there is no reason to perform the balanced model reduction procedure.

The first bound uses the Hankel singular values of the system. Corollary 9.3 in [12] states that

$$\|F(\omega, n)\|_{L^\infty} \leq 2(\sigma_1 + \sigma_2 + \cdots + \sigma_{N-1}). \tag{36}$$

Thus, if all of the singular values are known and twice their sum is still less than the maximum allowable magnitude response peak height, there is no need to continue the procedure and find a balanced model realization for the system.

Although the previous bound is guaranteed, it is often not very tight. In the FIR case, the authors have observed that the magnitude response peak of the single-state IIR approximate filter has a larger magnitude than the magnitude response peak of the true filter, that is

$$\|F(\omega, n)\|_{L^\infty} \leq \|F_1(\omega, n)\|_{L^\infty}. \tag{37}$$

This has been observed during simulations that included a wide variation in the number of filter weights, number of other peaks, peak location, and peak width. In all cases, this bound held for filters with large magnitude response peaks. This bound is attractive because the reduced-order filter is easily bounded. In [12], in the proof of Theorem 9.6, it is shown that

$$\|F_{i+1}(\omega, n) - F_i(\omega, n)\|_{L^\infty} \leq 2\sigma_{i+1}. \tag{38}$$

Taking $i = 0$ and noting that the $F_0(\omega, n) = b_0^*(n)$ gives

$$\|F(\omega, n)\|_{L^\infty} \leq 2\sigma_1 + |b_0|. \tag{39}$$

The magnitude of the first filter weight is easily obtained. The quantity σ_1 is the easiest singular value to obtain since it is the largest. A number of techniques exist for finding the largest eigenvalue of a matrix, and these techniques can be applied to $\mathbf{H}^H\mathbf{H}$ (see [24]). This approximation tends to be a reasonably close estimate of the magnitude response peak height and, therefore, tends to be a good indicator of when a full balanced realization of the system is needed.

One final bound does not require any singular values. Recall that the frequency response of an FIR filter with the tap-weight vector $\mathbf{w}(n)$ can be found at any frequency by finding the inner product of the filter tap weights with the frequency vector $\mathbf{s}(\omega)$. Extending this idea to the impulse response of an IIR filter $\{\zeta(k)\}$ (which corresponds to the weight vector of an equivalent infinite tap-weight FIR filter) and using the triangle inequality gives

$$\begin{aligned}\|F(\omega, n)\|_{L^\infty} &= \max_\omega |F(\omega, n)| = \max_\omega |\mathbf{f}^H(n)\mathbf{s}(\omega)| \\ &= \max_\omega \left| \sum_{k=0}^{\infty} \zeta^*(k) \exp(-jk\omega) \right| \\ &\leq \sum_{k=0}^{\infty} |\zeta(k)|. \end{aligned} \tag{40}$$

Thus, the sum of the absolute values of the impulse response forms an upper bound on the frequency response magnitude of the system. In the case of an FIR filter, the terms of the impulse response can be replaced with the tap weights $b_k(n)$.

VI. CASE STUDY

An example of the entire magnitude response peak detection and control process is now provided. Once a period, one of the symbols $1 + j, 1 - j, -1 + j$, and $-1 - j$ was randomly selected (with equal probability for each symbol) and sent over a channel with the frequency response shown by the dashed line in Fig. 1. Note that the channel response had several nulls of varying depth. The deepest null occurred at the normalized frequency of 1.4π rad/sample, where the channel had a response of zero. Other less severe nulls occurred at 0.9π, 0.4π, and 0.1π rad/sample. A small amount of noise was added to the signal between the channel output and the equalizer input. The equalizer consisted of a 101-tap FIR filter that was allowed to adapt using the standard LMS algorithm with $\mu = 0.001$. A threshold of 10 was selected. Occasionally, the operation of the system was stopped, and the current filter tap weights were examined. After 5000, 10 000, 20 000, 30 000, and 40 000 iterations, the current tap weights were temporarily frozen; therefore, a "snapshot" of the current frequency response of the filter could be formed. These frequency responses are shown in Fig. 1. Note how the peaks slowly grow at the frequencies of the channel nulls. The peak magnitude of each of these responses is shown in Table I. Every time the tap weights were frozen, the three frequency response magnitude bounds were calculated. They are also shown in Table I.

All three bounds on the magnitude response peak exceeded the preset threshold after 30 000 iterations. The maximum frequency response magnitude of the filter was less than 10, however, so no further steps were taken. After 40 000

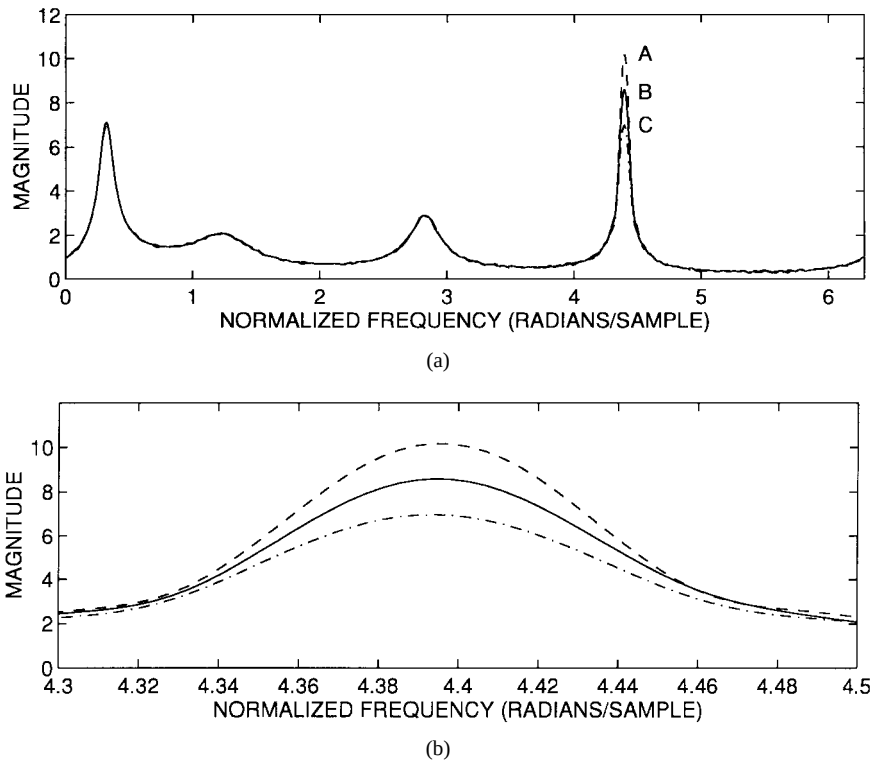

Fig. 2. Frequency responses of the equalizer at $n = 40\,000$ (A, dashed), target tap-weight vector (C, dash-dot), and the equalizer after 50 000 additional iterations using leakage to a target (B, solid). (a) All frequencies. (b) Frequencies near the magnitude response peak.

iterations, all three magnitude response peak bounds once again exceeded the threshold; therefore, a reduced order model was formed to check the maximum frequency response. To determine the equalizer's peak frequency response height, the upper left term in the $\mathbf{A}$ matrix of the balanced realization of the filter was examined. This value $-0.3009 - j0.9299$ corresponded to a normalized frequency of 1.4004π rad/sample. A frequency response vector was formed for this frequency and used to find the magnitude of the filter's response at this frequency. The result obtained, which was 10.1303, was slightly less than the true peak value of 10.1546, but it was still above the threshold of 10.

A target tap-weight vector was formed by adding a pole-zero pair to the $n = 40\,000$ tap weights. The pole and zero were placed at the normalized frequency of 1.4004π rad/sample at distances from the origin of 0.9417 and 0.9612, respectively. The frequency response of the resulting target tap-weight vector is shown along with the frequency response of the weight vector $\mathbf{w}(40\,000)$ in Fig. 2. The target frequency response had a peak height of 6.9877. Leakage to a target was now initiated with $\gamma = \gamma_i = 0.1 \forall i$. Adaptation was paused after 5000, 10 000, and 50 000 additional iterations to study the filter's frequency responses. After only 5000 iterations, the peak had been reduced to 9.3182. After 10 000 iterations, the peak magnitude was only 8.9450. A full 50 000 iterations reduced the peak only slightly further to 8.5535. Fig. 2 shows the frequency response of the filter after 50 000 iterations. (It should be noted that the tap-weight vector achieved after 50 000 iterations of LTAT was very close to the LTAT steady-state tap-weight vector.)

Fig. 3 shows the steady-state frequency responses for standard LMS (which is the MMSE frequency response), LTAT, and leakage (with γ kept at 0.1). In addition, the steady-state response of a third magnitude response peak reduction procedure is shown. In this procedure, the desired signal was filtered so that it had no power at the magnitude response peak frequency, and standard LMS was used to adapt the weights. In this case, a 21-weight notch filter was used to remove the desired signal energy at 1.4004π rad/sample. For frequencies other than the magnitude response peak frequency, the MMSE, LTAT, and filtered desired signal algorithm responses are nearly identical, whereas the leakage response is noticeably different at most frequencies. The MSE for each of these tap-weight vectors was now calculated. The MMSE was 0.020, the LTAT steady-state MSE was 0.026, the leakage steady-state MSE was 0.091, and the filtered desired signal algorithm MSE was 0.109. Thus, LTAT caused 30% additional MSE (above the MMSE), whereas leakage caused 355% additional MSE (or approximately 11.8 times more than LTAT), and the filtered desired signal algorithm caused 445% additional MSE (or approximately 14.8 times more than LTAT).

To study the effect of LTAT on an equalizer's ability to adapt to a time varying channel, the channel was modified somewhat, and the new steady-state frequency responses were examined. For the new channel, the deepest null was moved to 1.3π rad/sample, and the null at 0.9π rad/sample was moved to 0.8π rad/sample and shallowed out somewhat. The new steady-state frequency responses are plotted in Fig. 4. The LTAT response is fairly close to the MMSE response, except at the new magnitude response peak frequency, where the LTAT magnitude

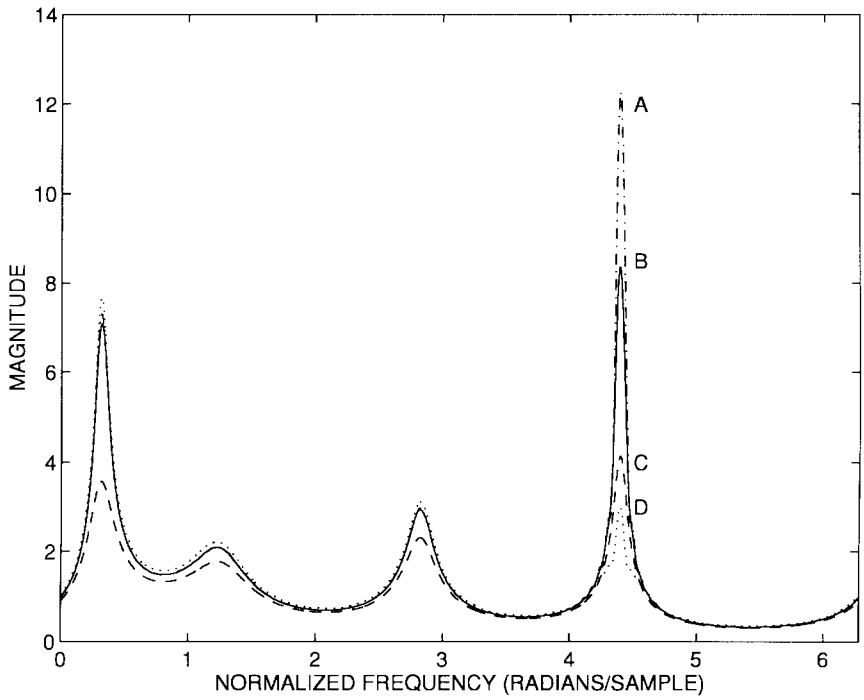

Fig. 3. Steady-state equalizer responses: MMSE (A, dash-dot), LTAT (B, solid), leakage (C, dashed), and filtered desired signal (D, dotted).

is under 5, whereas the MMSE magnitude is over 12. The leakage response roughly approximates the MMSE response except in the peaks. The response of the algorithm utilizing a filtered desired signal is fairly close to the MMSE response at all frequencies, including the new magnitude response peak frequency, where it had an unacceptable magnitude of 11.95. The new MSE values were 0.020 for the MMSE response, 0.062 for LTAT (210% additional MSE), 0.097 for leakage (385% additional MSE), and 0.122 for the filtered desired signal algorithm (510% additional MSE). Thus, filtering the desired signal did not prevent a magnitude response peak from forming when the channel null moved slightly while leakage, and LTAT did prevent a new peak from forming. Leakage, however, caused a significantly larger amount of MSE than LTAT. By lowering γ, the response of the filter to a time-varying channel could be improved in the case of LTAT. Lowering γ would have the effect of reducing the "pull" of the target that was designed for the original channel. Changing γ, however, would also effect how effectively the filter leaks off dangerous magnitude response peaks.

VII. Conclusions

This paper shows that magnitude response peaks can be detected using a balanced model reduction procedure and that magnitude response peaks can be controlled using leakage to a target. The balanced model reduction procedure produces a single state IIR filter with pole placed at the frequency of the largest magnitude response peak. Leakage to a target biases the equalizer frequency response away from the minimum mean-squared error frequency response and toward a target frequency response selected to concentrate the effect of the leakage on the region of the magnitude response peak. A well-chosen target vector and leakage factor will reduce magnitude response peaks without significantly increasing the mean-squared error of the filter. In addition, LTAT prevents new magnitude response peaks from forming in a filter's response due to a time-varying channel.

In several potential applications of this procedure, fractionally spaced equalizers, and acoustical systems, the region where magnitude response peaks may form is known beforehand. In these applications, it is possible to bypass the peak detection process and design a target tap-weight vector that could successfully control a peak at any frequency in the underexcited region.

Appendix A
Minimum Mean-Squared Error Eigenfilter Weights

The minimum mean-squared eigenfilter weights for an FIR filter can be expressed as weighted projections of the unrestrained (any order) optimal filter's tap-weight vector onto the eigenvectors of the input autocorrelation. Any finite dimensional tap-weight vector $\mathbf{h}$ can be written as an infinite tap-weight vector by adding zeros. $\overline{\mathbf{h}} = [\mathbf{h}^T, 0, 0, \cdots]^T$. The infinite filter input vector is $\overline{\mathbf{u}}(n) = [x(n), x(n-1), \cdots]^T$, and its infinite autocorrelation, assuming stationarity, is $\overline{\mathbf{R}} = E[\overline{\mathbf{u}}(n)\overline{\mathbf{u}}^H(n)]$. Using the infinite input vector, the desired signal can be written in terms of the unrestrained (any order) optimal tap-weight vector $\overline{\mathbf{g}}$ as $d(n) = \overline{\mathbf{g}}^H\overline{\mathbf{u}}(n)$. An inner product between filters excited by the input process $\{u(n)\}$ can be defined in terms of impulse response vectors as

$$\langle \mathbf{h}_1, \mathbf{h}_2 \rangle_u \equiv \overline{\mathbf{h}}_2^H \overline{\mathbf{R}} \overline{\mathbf{h}}_1. \tag{41}$$

This quantity is an inner product due to the linearity of matrix multiplication and the assumption that the autocorrelation

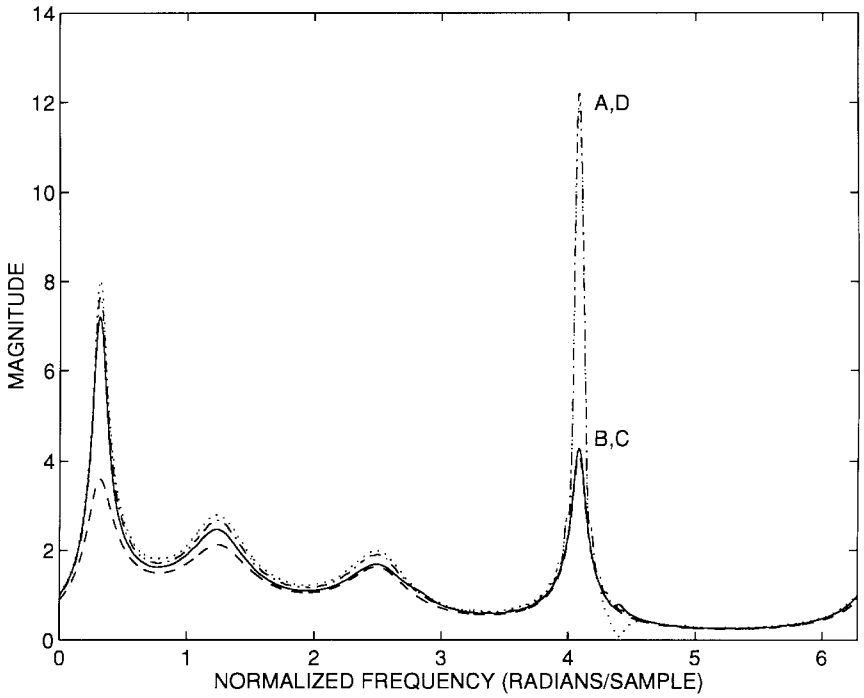

Fig. 4. Steady-state equalizer responses for a new channel: MMSE (A, dash-dot), LTAT (B, solid), leakage (C, dashed), and filtered desired signal (D, dotted).

matrix is positive definite. This norm has the desirable property that $\langle \mathbf{v}_i, \mathbf{v}_j \rangle_u = \lambda_i \delta_{ij}$. Applying Theorem 1 shows that

$$F_i^o = \frac{\mathbf{p}^H \mathbf{v}_i}{\lambda_i} = \frac{E[d(n)\mathbf{u}^H(n)]\mathbf{v}_i}{\lambda_i} = \frac{\overline{\mathbf{g}}^H \overline{\mathbf{R}} \overline{\mathbf{v}}_i}{\lambda_i} = \frac{\langle \mathbf{v}_i, \mathbf{g} \rangle_u}{\lambda_i}. \tag{42}$$

This result can also be found using vector space optimization techniques by writing the mean-squared error associated with a tap-weight vector $\mathbf{h}$ in terms of the norm.

$$\begin{aligned} E[|e(n)|^2] &= E[|d(n) - y(n)|^2] \\ &= E[|\overline{\mathbf{g}}^H \overline{\mathbf{u}}(n) - \overline{\mathbf{h}}^H \overline{\mathbf{u}}(n)|^2] \\ &= E\{[(\overline{\mathbf{g}}^H - \overline{\mathbf{h}}^H)\overline{\mathbf{u}}(n)] \cdot [(\overline{\mathbf{g}}^H - \overline{\mathbf{h}}^H)\overline{\mathbf{u}}(n)]^*\} \\ &= (\overline{\mathbf{g}}^H - \overline{\mathbf{h}}^H) \cdot \overline{\mathbf{R}} \cdot (\overline{\mathbf{g}} - \overline{\mathbf{h}}) = \|\overline{\mathbf{g}} - \overline{\mathbf{h}}\|_u^2. \end{aligned} \tag{43}$$

Defining $\mathcal{T}$ to be the set of length N tap-weight vectors, the minimization problem becomes

$$\mathbf{w}_o = \underset{\mathbf{h} \in \mathcal{T}}{\operatorname{argmin}} E[|e(n)|^2] = \underset{\mathbf{h} \in \mathcal{T}}{\operatorname{argmin}} \|\overline{\mathbf{g}} - \overline{\mathbf{h}}\|_u^2. \tag{44}$$

Since all the eigenvectors can be considered N-dimensional tap-weight vectors, they all lie in $\mathcal{T}$. Thus, by the projection theorem, the difference $\overline{\mathbf{g}} - \overline{\mathbf{w}}_o$ must be orthogonal to $\mathcal{T}$. Therefore, $\forall i$, $\langle \overline{\mathbf{g}} - \overline{\mathbf{w}}_o, \mathbf{v}_i \rangle_u = 0$. Rearranging

$$\begin{aligned} \langle \mathbf{g}, \mathbf{v}_i \rangle_u = \langle \mathbf{w}_o, \mathbf{v}_i \rangle_u &= \left\langle \sum_{j=0}^{N-1} F_j^{o*} \mathbf{v}_j, \mathbf{v}_i \right\rangle_u \\ &= \sum_{j=0}^{N-1} F_j^{o*} \langle \mathbf{v}_j, \mathbf{v}_i \rangle_u = \sum_{j=0}^{N-1} F_j^{o*} \lambda_i \delta_{ij} \\ &= \lambda_i F_j^{o*}. \end{aligned} \tag{45}$$

This gives $F_i^o = \langle \mathbf{v}_i, \mathbf{g} \rangle_u / \lambda_i$, as before.

Similar results can be found in the frequency domain as in [22] and [23]. Defining the inner product of any two filter frequency responses excited by the input process $\{u(n)\}$ as

$$\langle H_1(\omega), H_2(\omega) \rangle_u \equiv \frac{1}{2\pi} \int_{-\pi}^{\pi} H_1(\omega) S_{uu}(\omega) H_2^*(\omega)\, d\omega \tag{46}$$

vector space optimization techniques can be used to show

$$\begin{aligned} F_i^o &= \frac{\langle G(\omega), V_i(\omega) \rangle_u}{\lambda_i} \\ &= \frac{1}{2\pi\lambda_i} \int_{-\pi}^{\pi} G(\omega) S_{uu}(\omega) V_i^*(\omega)\, d\omega \end{aligned} \tag{47}$$

where the inner products in (41) and (46) differ only by a conjugate.

REFERENCES

[1] W. A. Sethares, D. A. Lawrence, C. R. Johnson, and R. R. Bitmead, "Parameter drift in LMS adaptive filters," *IEEE Trans. Acoust., Speech, Signal Processing*, vol. ASSP-34, pp. 868–879, Aug. 1986.

[2] J. M. Cioffi, "Limited-precision effects in adaptive filtering," *IEEE Trans. Circuits Syst.*, vol. CAS-34, pp. 821–833, July 1987.

[3] G. Ungerboeck, "Fractional tap-spacing equalizer and consequences for clock recovery in data modems," *IEEE Trans. Commun.*, vol. COMM-24, pp. 856–864, Aug. 1976.

[4] R. D. Gitlin, H. C. Meadors, Jr., and S. B. Weinstein, "The tap-leakage algorithm: An algorithm for the stable operation of a digitally implemented, fractionally spaced adaptive equalizer," *Bell Syst. Tech. J.*, vol. 61, no. 8, pp. 1817–1839, Oct. 1982.

[5] L. A. Poole, G. E. Warnaka, and R. C. Cutter, "The implementation of digital filters using a modified Widrow–Hoff algorithm for the adaptive cancellation of acoustic noise," in *Proc. IEEE 1984 Conf. Acoust., Speech, Signal Processing, ICASSP*, San Diego, CA, Mar. 1984, pp. 21.7.1–21.7.4.

[6] J. Tichy, "Active systems for sound attenuation in ducts," in *Proc. IEEE 1988 Conf. Acoust., Speech, Signal Processing, ICASSP*, New York, Apr. 1988, pp. 2602–2605.

[7] J. G. Proakis and J. H. Miller, "An adaptive receiver for digital signaling through channels with intersymbol interference," *IEEE Trans. Inform. Theory*, vol. IT-15, pp. 484–497, July 1969.

[8] S. U. H. Qureshi, "Adaptive equalization," *Proc. IEEE*, vol. 73, pp. 1349–1387, Sept. 1985.
[9] C. R. Johnson, Jr., *Lectures on Adaptive Parameter Estimation.* Englewood Cliffs, NJ: Prentice-Hall, 1988.
[10] B. D. O. Anderson and C. R. Johnson, Jr., "Exponential convergence of adaptive identification and control algorithms," *Automatica*, vol. 18, no. 1, pp. 1–13, Jan. 1982.
[11] B. C. Moore, "Principal component analysis in linear systems: Controllability, observability, and model reduction," *IEEE Trans. Automat. Contr.*, vol. AC-26, pp. 17–32, Feb. 1981.
[12] K. Glover, "All optimal Hankel–Norm approximations of linear multivariable systems and their L^{∞}-error bounds," *Int. J. Contr.*, vol. 39, no. 6, pp. 1115–1193, June 1984.
[13] M. Green and D. J. N. Limebeer, *Linear Robust Control.* Englewood Cliffs, NJ: Prentice-Hall, 1995.
[14] A. J. Laub, "Computation of 'balancing' transformations," in *Proc. 1980 Joint Automat. Contr. Conf.*, San Francisco, CA, Aug. 1980.
[15] A. J. Laub, M. T. Heath, C. C. Paige, and R. C. Ward, "Computation of system balancing transformations and other applications of simultaneous diagonalization algorithms," *IEEE Trans. Automat. Contr.*, vol. AC-32, pp. 115–121, Feb. 1987.
[16] B. Beliczynski, I. Kale, and G. D. Cain, "Approximation of FIR by IIR digital filters: An algorithm based on balanced model reduction," *IEEE Trans. Signal Processing*, vol. 40, pp. 532–542, Mar. 1992.
[17] J. J. Dongarra, C. B. Moler, J. R. Bunch, and G. W. Stewart, *LINPACK User's Guide.* Philadelphia, PA: SIAM, 1979.
[18] G. H. Golub and C. F. Van Loan, *Matrix Computations.* Baltimore, MD: Johns Hopkins Univ. Press, 1989.
[19] S. Haykin, *Adaptive Filter Theory*, 2nd ed. Englewood Cliffs, NJ: Prentice-Hall, 1991.
[20] W. A. Sethares, "The least mean square family," in *Adaptive System Identification and Signal Processing Algorithms*, N. Kalouptsidis and S. Theodoridis, Eds. London, U.K.: Prentice-Hall Int., 1993.
[21] C. L. Zahm, "Application of adaptive arrays to suppress strong jammers in the presence of weak signals," *IEEE Trans. Aerosp. Electron. Syst.*, vol. AES-9, pp. 260–271, Mar. 1973.
[22] C. Johnson, Jr., B. Egardt, and G. Kubin, "Frequency-domain interpretation of LMS performance," submitted for publication.
[23] G. Kubin, C. R. Johnson, Jr., and B. Egardt, "Frequency-domain bias decomposition for LMS and LS adaptive filters," in *Proc. IEEE 1993 Conf. Acoust., Speech, Signal Processing, ICASSP* Minneapolis, MN, Apr. 1993, pp. 531–534.
[24] R. G. Stanton, *Numerical Methods for Science and Engineering.* Englewood Cliffs, NJ: Prentice-Hall, 1961.

Kent D. Benson (S'89) was born in Ames, IA, in 1968. He received the B.S. degree in electrical engineering from Iowa State University, Ames, in 1991 and the M.S. and Ph.D. degrees in electrical engineering from the University of Wisconsin, Madison, in 1993 and 1997, respectively.

While at the University of Wisconsin, he was a Lecturer in the Department of Electrical and Computer Engineering. Since 1997, he has been a Research Engineer with Tellabs Operations, Inc., Mishawaka, IN. His research interests include adaptive signal processing and control as well as communications systems.

William A. Sethares received the B.A. degree in mathematics from Brandeis University, Waltham, MA, and the M.S. and Ph.D. degrees in electrical engineering from Cornell University, Ithaca, NY.

He has worked at Raytheon Company as a Systems Engineer and is currently Associate Professor in the Department of Electrical and Computer Engineering at the University of Wisconsin, Madison. His research interests include signal processing, communications, and acoustics. He is the author of *Tuning, Timbre, Spectrum, Scale*.